

# CHEMICAL ANALYSIS IN THE GEMOLOGICAL LABORATORY: XRF AND LA-ICP-MS

Zi Yin Sun, Michael Jollands, and Aaron C. Palke

The modern gem trade faces challenges that require sophisticated analytical instrumentation beyond what was needed in the early days of gemological laboratories. Several identification problems can only be solved through precise measurements of the chemical composition of a gemstone. The two techniques used most commonly in an advanced gemological laboratory are energy-dispersive X-ray fluorescence (EDXRF, or XRF) and laser ablation–inductively coupled plasma–mass spectrometry (LA-ICP-MS). XRF was initially introduced for general identification purposes and detection of some treatments such as lead glass filling in rubies. LA-ICP-MS, a much more sensitive technique, emerged in the detection of beryllium-diffused sapphires but has become an invaluable tool for determining the geographic origin of many colored stones. This contribution provides a technical overview of both techniques and presents several examples of how they are employed in the laboratory for gemstone identification.

This contribution describes two analytical techniques: X-ray fluorescence (XRF) and laser ablation–inductively coupled plasma–mass spectrometry (LA-ICP-MS). Both are instrumental in gemological testing, as they enable the chemical composition of a stone (usually a colored stone) to be determined either nondestructively (XRF) or by sampling only minimal amounts of the stone (LA-ICP-MS). These analytical methods are essential tools in the modern gemological laboratory for gemstone identification, geographic origin determination, and detecting certain treatments. With XRF, a gemstone is bombarded with high-energy X-rays, causing the atoms in the stone to emit characteristic X-rays that can be measured with a spectrometer to establish its elemental composition. LA-ICP-MS uses a focused laser to microsample a gemstone (typically on the girdle) with a very small amount of material delivered into an inductively coupled plasma (ICP) and then transferred into a mass spectrometer (MS) for chemical analysis. LA-ICP-MS offers greater sensitivity, lower detection limits, and the capacity to detect a wider range of elements (including those lighter than sodium). The laser-induced breakdown spectroscopy (LIBS) technique will also be briefly introduced. LIBS

and LA-ICP-MS are both microanalytical techniques, and the two share some similarities.

Together, XRF and LA-ICP-MS form a powerful arsenal for gemologists seeking to unravel the chemical mysteries of some of the world's most captivating gemstones. Whether used singly or in combination, these techniques have vastly expanded our knowledge of gemstone composition, provenance, and treatment history, and they will undoubtedly continue to play a pivotal role in advancing the field of gemological research.

## TECHNICAL BACKGROUND

**X-Ray Fluorescence (XRF) Spectrometry.** This was one of the first chemical analysis techniques adopted by gemological laboratories. Prior to the 1980s, standard gemological testing was generally sufficient for routine gem species identification. However, as new challenges arose—distinguishing natural from synthetic stones, detecting lead glass filling in rubies, and separating low- and high-iron rubies for origin determination, to name a few—gemological laboratories needed to expand their analytical capabilities to include measurement of a stone's chemical composition. XRF spectrometers were introduced to gemological labs in the 1980s and were, at the time, the most accessible instruments for conducting non-destructive chemical testing of gemstones.

X-rays are electromagnetic waves with short wavelength and high energy, falling between ultra-

---

See end of article for About the Authors and Acknowledgments.

GEMS & GEMOLOGY, Vol. 60, No. 4, pp. 536–559,

<http://dx.doi.org/10.5741/GEMS.60.4.536>

© 2024 Gemological Institute of America

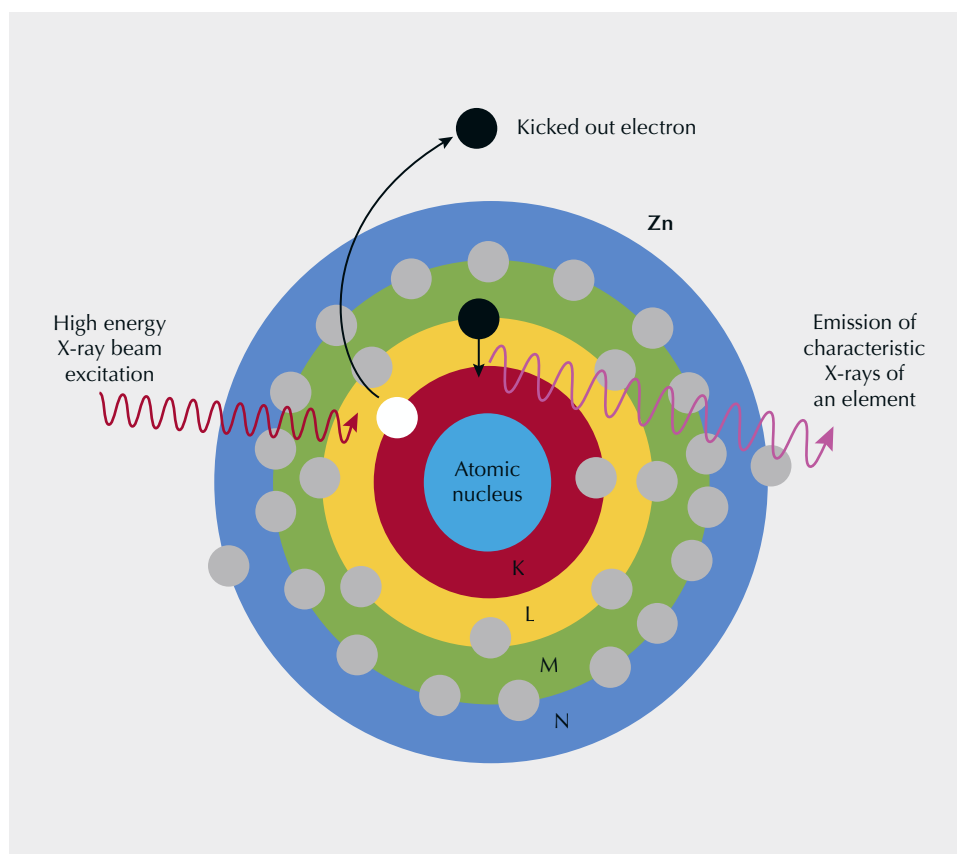


Figure 1. The principle of fluorescent X-ray emission. An X-ray tube directs high-energy X-rays at the sample, some of which penetrate atoms in the sample and can knock out inner-shell electrons. These atoms then emit characteristic X-rays when an outer-shell electron falls in to replace the ejected electron. These characteristic X-rays can be measured to fingerprint the elements present in the sample.

violet rays and gamma rays on the electromagnetic spectrum. In an XRF unit, a sample such as a gemstone is bombarded with a stream of X-rays generated by passing a current through a metal filament, which then emits electrons that are accelerated toward a metal target, often rhodium, molybdenum, tungsten, or copper. When the electrons strike this metal target, it emits a stream of X-rays directed at the gemstone to be analyzed. The X-rays are usually directed at the table of a faceted stone or either the dome or base of a cabochon. Upon striking the gem's surface, the X-rays interact with its constituent atoms. While many of the X-rays are scattered away, some will penetrate into the inner electron shells of the atoms, knocking out an electron (as long as the incident X-ray has energy greater than the binding energy of these inner electrons) (figure 1). This creates an electron hole, which is then filled by an electron from an outer electron shell. Each electron shell in an atom has a discrete, well-defined energy level. When an outer shell electron falls into an inner shell, it releases energy in the form of an X-ray whose energy corresponds to the difference in energy levels between the two shells. This phenomenon is known as fluorescence

and is similar, at least in principle, to photoluminescence, described by Eaton-Magaña et al. (2024), pp. 494–517 of this issue.

Each atom has a unique “fingerprint” of electron shell energy levels. This means that each type of atom in a material will emit its own characteristic

### In Brief

- Many geological questions require accurate and precise measurements of a gemstone's chemistry.
- X-ray fluorescence spectroscopy is a relatively simple technique to measure chemistry, but it has largely been supplanted by laser ablation–inductively coupled plasma–mass spectrometry, which has better precision and measures a wider range of elements.
- While both techniques are used in identification challenges, one main focus for chemical measurements is geographic origin determination.

pattern (spectrum) of X-rays corresponding to the differences in energy levels between its inner and outer electron shells. In other words, the pattern of energies (or wavelengths) of emitted X-rays measured by an

## BOX A: PORTABLE XRF DEVICES

Since XRF was first used for elemental analysis in 1913, the technology and the device have continued to advance. Around the mid-1960s, portable XRF devices started to enter the market. The early versions consisted of at least two units: a probe with a measurement head and a processing/display unit connected to the probe. Although these instruments still lacked true mobility and a user-friendly interface, they did allow for on-site analyses with reasonable results. Industries began to realize that this category of devices could lower the cost of sampling, transportation, and analyzing, reducing operational downtime.

With increasing demand from multiple industries, the first fully handheld single-unit XRF analyzer was introduced in 1994. Niton, which later became part of Thermo Fisher Scientific, released the XL-309. This device weighed only 1.13 kg (2.5 lbs.) and featured enhanced analytical performance, at a much lower price point than its predecessors.

With the publication of the U.S. Environmental Protection Agency's Standard Method 6200 in 1996, field-portable XRF was recognized as an elemental analytical method. Since then, the portable XRF landscape has

evolved rapidly. Miniaturized X-ray tubes have replaced radioactive isotope emitters to make portable devices much smaller, more affordable, better-performing, and safer. Desktop and handheld devices alike are widely applied in numerous industries: mining, agriculture, art conservation, archaeology, forensics, petroleum, aerospace, nanotechnology, food and beverage, consumer goods, and jewelry, to name a few.

As the demand for portable XRF units continues to grow and new markets develop globally, nearly all instrumentation companies offer their own product line. Key players in this field include Thermo Fisher Scientific, Bruker, Rigaku, Olympus, Fischer Technologies, Shimadzu, Spectro Analytical Instruments, Horiba, Hitachi High-Tech, and Oxford Instruments. These manufacturers offer multiple models of portable XRF devices to cater to different users. The price of a unit today can range from thousands to tens of thousands of U.S. dollars. While most portable devices are not designed specifically for the gem and jewelry industry, many can easily tackle precious metal analysis and be adapted to gem identification.



*Figure A-1. The Horiba Mesa-50 XRF is used by GIA's laboratories. Gemstones and jewelry pieces can be placed on top of the testing window. A laptop is connected to the testing unit, and the system also has a built-in camera that allows the user to adjust the position of the X-ray beam on the sample. Photo by Kevin Schumacher.*





Figure A-2. The Thermo Scientific Niton XL2 is the portable XRF device used by GIA to quickly test precious metals. Photo by Emily Lane; courtesy of Hallock Coin.

One key consideration in using a portable XRF apparatus is safety. Regulations on X-ray usage can vary by country and jurisdiction. Before buying and using any X-ray generating device, a user must complete required training and adopt defined safety protocols. If using these devices for teaching or allowing others to operate them, the required training and protection must be provided.

One of the units at GIA is the Horiba Mesa-50, a compact desktop XRF that can be moved from one place to another or transported off-site if needed (figure A-1). Instruments like this are designed to be very user-friendly. There is no sample preparation required other than cleaning the surface. Many of these instruments have built-in cameras to allow users to target a specific area of the material being tested. The use of the fundamental parameters method for calculating concentrations further streamlines

operations and allows data to be collected without the use of external standards, which can yield greater accuracy but are cumbersome to set up and may be unnecessary for routine identification and characterization. These desktop instruments share many of the same capabilities as more robust lab units, including detection of silver in color-treated pearls, detection of coatings on zoisite, and gemstone identification, among others. The Horiba Mesa-50 also has a “recipe” procedure where users can quickly create new methods and train them with known samples for rapid identification. Some disadvantages of desktop units include their inability to draw a vacuum in the sample chamber and the weaker signals produced from the analyzed gemstones.

In recent years, companies have released compact, handheld XRF units designed for field use. Of particular interest for the gem and jewelry industry are handheld XRF units optimized for precious metals testing, allowing rapid measurement of gold, silver, and platinum contents in jewelry in an office setting or in the field (figure A-2).

#### CHECKLIST FOR PURCHASING A PORTABLE XRF DEVICE

##### Self-Assessment

- Do I need elemental analysis for my precious metals and gemstones?
- What types of elements do I need to detect or analyze?
- What detection limit is needed for the elements I want to focus on?
- Do I have the ability to build a database for gem identification?
- What is the mobility requirement of this device?
- What is my budget?

##### Questions for the Manufacturer

- What is the device designed for?
- What types of samples can be tested?
- Is special sample preparation needed?
- What is the lightest element the device can analyze?
- What is the safety standard of the device?

##### Additional Reading

[https://www.portaspecs.com/the-evolution-of-portable-xrf-instruments/\(timeline-of-portable-XRF\)](https://www.portaspecs.com/the-evolution-of-portable-xrf-instruments/(timeline-of-portable-XRF))  
<https://www.azonano.com/article.aspx?ArticleID=6531>  
<https://www.thermofisher.com/blog/materials/understanding-the-journey-from-lab-based-to-handheld-xrf-technology>

XRF is specific to each element. By measuring the X-ray energies across a broad energy range, one can identify not only single elements but also the majority of elements that make up a gem (excluding very light elements; see below). Most XRF systems use a type of detector that sorts X-rays by their energy, and this is known as an energy-dispersive XRF (EDXRF). The output is a spectrum plot with energy on the x-axis and intensity on the y-axis. Taking this a step further, the intensities of the peaks are proportional to the concentrations of those elements. Higher relative fluorescence intensity indicates a higher concentration, enabling quantitative analysis of the elements (Johnson and King, 1987). By calibrating the XRF detector using well-characterized reference standards, it is possible to quantify the concentrations of various major and minor trace elements in an unknown material. While most XRF units are desktop units, several portable and even handheld units are available in the market. These are often used on-site in mining or industrial applications or in jewelry stores or pawn shops for precious metals testing (box A).

EDXRF can measure most elements in the periodic table either semiquantitatively or quantitatively. However, it cannot measure elements with an atomic number less than 11, that of sodium. For instance, EDXRF cannot detect beryllium in corundum (He and Van Espen, 1991). A related technique, wavelength-dispersive XRF (WDXRF), is able to measure beryllium, at least at higher concentrations in the wt.% range, but these instruments are less efficient and more costly than EDXRF systems. For the remainder of this paper, "XRF" will refer specifically to EDXRF. The XRF instruments typically found in gemological laboratories consist of an X-ray generator, a sample chamber, a detector, and a data processing system that outputs the concentrations of measurable elements in the sample. XRF can measure lighter elements from magnesium to calcium in the wt.% range, transition metals around the 0.1 wt.% range, and many heavier elements down to the 0.01 wt.% range.

**Micro-Analytical Techniques for Gemstone Trace Element Chemistry: LA-ICP-MS.** The term *LA-ICP-MS* describes two separate but interconnected parts of a system. "LA" stands for laser ablation, a technique that allows very small amounts of material to be removed from a sample. This can be thought of as a micrometer-scale microdrill, but with the physical drill bit replaced by a pulsing laser. "ICP-MS" stands for inductively coupled plasma-mass spectrometry, which determines the chemical composition of the

ablated material by atomizing and ionizing it in a plasma and filtering the charged particles by mass through a mass spectrometer.

ICP-MS systems first became commercially available in the early 1980s, and the first demonstration of coupling ICP-MS to a laser ablation system followed shortly after (Gray, 1985). Since then, the technique has improved continuously (Sylvester and Jackson, 2016), although the fundamental concept remains basically the same. The lasers now use shorter, faster pulses of light with shorter wavelengths and higher energy. Different carrier gases are used, while optical components and sample holding methods have been modified. With these refinements, ICP-MS systems have been improved to maximize, among other factors, speed and sensitivity.

The LA-ICP-MS technique was adopted by gemological laboratories in the early 2000s. This was driven largely by the need to detect beryllium in response to the emerging problem of beryllium-diffused corundum (Emmett et al., 2003). Until then, the most common microanalytical technique applied to gemstones was electron probe microanalysis (EPMA) (e.g., Rinaldi and Llovet, 2015). EPMA is similar in principle to XRF, but with a focused electron beam as the excitation source for obtaining characteristic X-rays from the sample. Applications of LA-ICP-MS have since expanded to include such treatments as cobalt diffusion of spinel (Saeseaw et al., 2015) and, significantly, geographic origin determination (Pornwilard et al., 2011; Palke et al., 2019 a,b).

For similar reasons, the related technique of LIBS was being adopted in gemological testing at about the same time (Krzemnicki et al., 2004, 2006; McMillan et al., 2006). In this method, the laser ablation system is not interfaced to an ICP-MS. Rather, the small amount of light created as a result of the laser ablation is recorded using an optical spectrometer. The wavelengths of this emitted light can be used to determine, at least in part, the composition of the stone.

Colored stones submitted for analysis to a major gemological laboratory such as GIA often undergo LA-ICP-MS. The only evidence of this analysis consists of small holes, normally placed on the girdle and generally tens of micrometers wide and a few micrometers deep, that are essentially invisible to the unaided eye (figure 2). In the following section, we describe the complex analysis process and the vast amount of information that can be revealed.

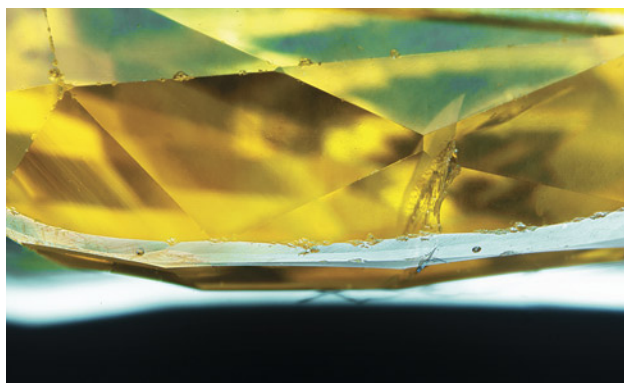


*Figure 2. The appearance of laser ablation spots on a faceted yellow sapphire. There are two ablation pits on the girdle, located left and right of center. They are 55  $\mu\text{m}$  in diameter and essentially undetectable without a microscope or loupe. Photomicrograph by Aaron Palke; field of view 5.21 mm.*

**How Do LA-ICP-MS Systems Work?** Starting with the LA system, the laser is its most important component. The lasers typically used in modern laser ablation systems for LA-ICP-MS operate in the ultraviolet range, using 193, 213, or 266 nm light. The latter two are solid-state lasers produced using a crystal medium and additional frequency-doubling crystals, while the former is generated from a precise and potentially hazardous mix of gases containing fluorine. The 213 nm systems provide a compromise between ablation quality (generally better at shorter

wavelengths) and user-friendliness (better at longer wavelengths), and these are used at GIA's global laboratories. Figure 3 shows the laser head of one of these systems. It houses a Nd:YAG laser rod inside a xenon flash lamp that uses ultraviolet light to stimulate fluorescence in the laser rod. Nd:YAG can produce intense infrared light with a wavelength of 1064 nm, which is then frequency-quintupled (i.e., the frequency is increased by a factor of five and the wavelength decreased by the same factor) to a wavelength of 213 nm using special nonlinear optical crystals.

The laser light is then passed through an optical channel consisting of a series of mirrors, lenses, apertures, and other optical components. The last part of the optical channel is a microscope objective, which focuses the beam onto the sample. The optical channel creates a small (tens of micrometers), well-defined beam of light that can ablate material from the sample.

The samples are loaded into a cell (effectively a closed box) that has a controlled stream of gas, usually pure helium, flowing in and out. The cells used in gemstone analysis must be deep enough to hold large, loose stones or even mounted jewelry.

The laser is then focused onto the surface of the stone and pulsed, typically between 5 and 20 Hz (pulses per second). When the laser strikes the sample with high enough energy, ablation will occur. In other words, the bonds holding the atoms together in the crystal can be broken, allowing the atoms to

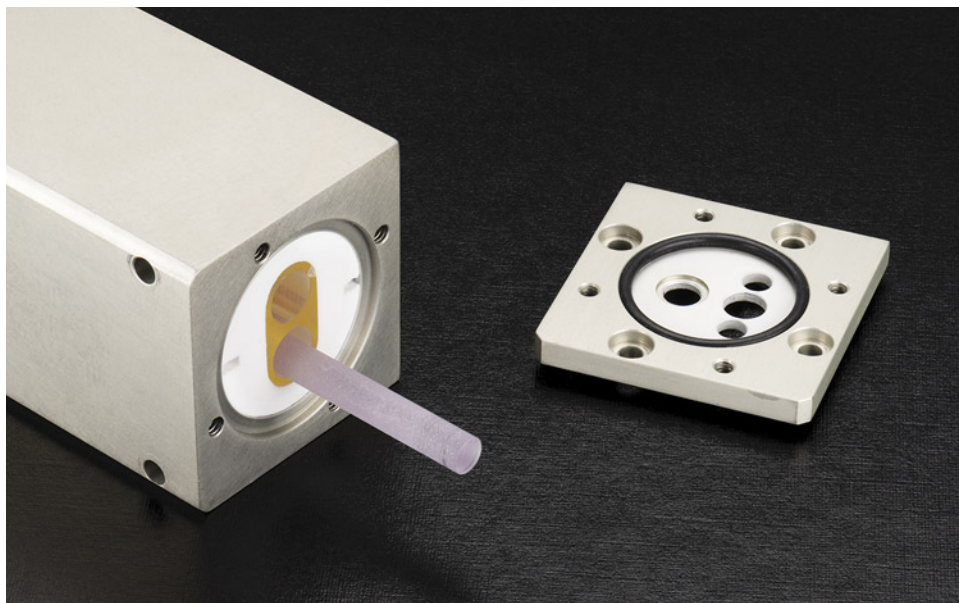


*Figure 3. The laser head of one of the 213 nm laser ablation systems used at GIA. In this system, a Nd:YAG rod is housed in a chamber along with a xenon flash lamp that stimulates the production of 1064 nm fluorescence from the Nd:YAG. This fluorescence is frequency-quintupled to 213 nm light and focused into a laser. Photo by Emily Lane.*



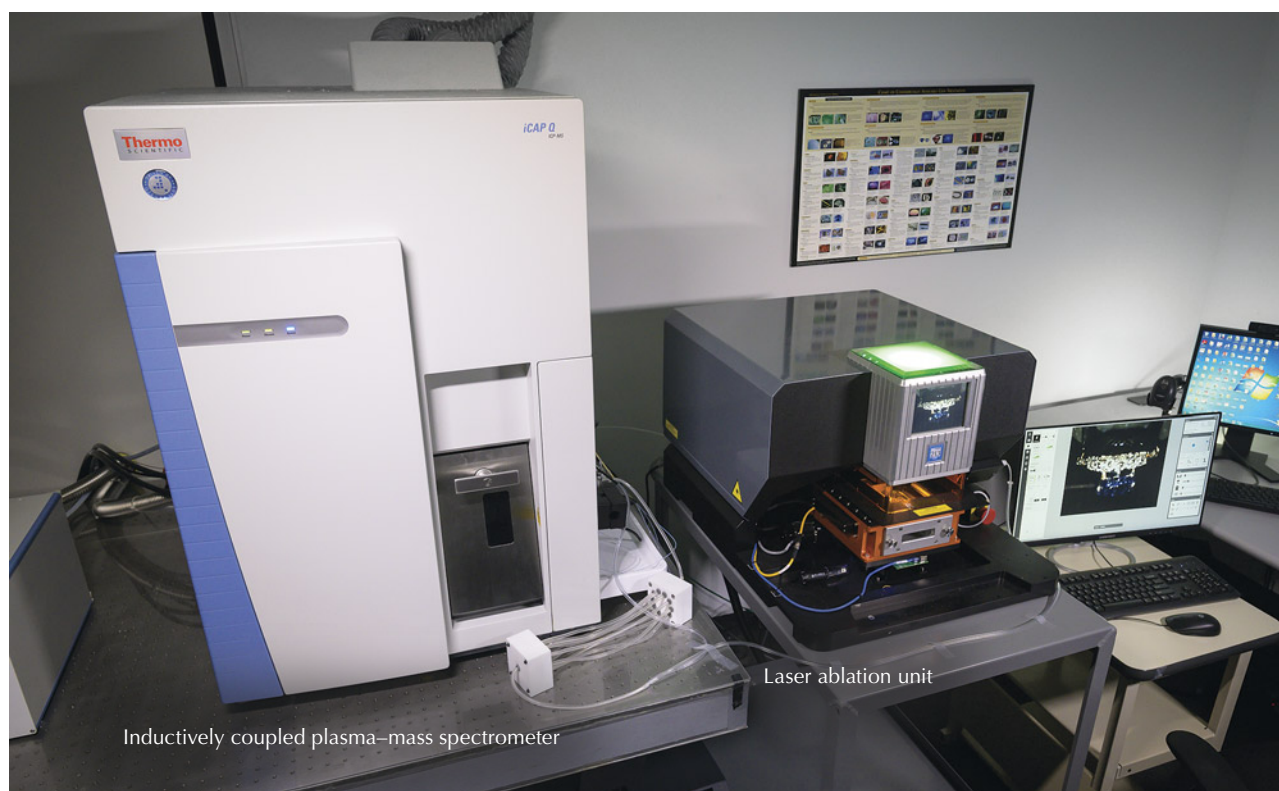


Figure 4. The LA-ICP-MS system at GIA's Carlsbad laboratory, consisting of a New Wave Research ESI NWR 213 laser ablation system and a Thermo Fisher Scientific iCAP-Q inductively coupled plasma-mass spectrometer. Photo by Kevin Schumacher.

be freed from the solid. These evaporated atoms form a plasma, which can be considered a highly energetic gas. As the plasma loses energy, the ablated material condenses into droplets that are rapidly swept away from the site of ablation by the helium carrier gas, toward the ICP-MS.

The helium is generally mixed with argon gas and passed together into an argon plasma (the ICP), which converts the material coming from the laser into ions. This ionization is necessary because the mass spectrometer does not measure mass, but rather the ratio of mass to charge. This means that an electron, or multiple electrons, must be stripped from the atoms being analyzed. The ionized material from the plasma, which is at atmospheric pressure, then moves through small orifices into the high-vacuum body of the mass spectrometer.

At this point, the stream of ions of ablated material also contains contaminants such as nitrogen, oxygen, and carbon from the atmosphere and argon from the plasma. The next step is to separate the ions based on their mass-to-charge ratio, which is accomplished in most LA-ICP-MS systems used in gemological laboratories through a quadrupole mass analyzer. The

quadrupole consists of four cylindrical rods that selectively allow only species with a certain mass-to-charge ratio to pass through, by applying oscillating electric fields. Ions that are too heavy or too light are filtered out. Ions that have successfully passed through the quadrupole are then detected, typically with an "electron multiplier" that converts the number of ions that have exited the quadrupole into an electrical current, which can be recorded by a computer.

As with XRF, periodically analyzing materials with well-known concentrations (i.e., standards) establishes the relationship between the recorded signal and the concentration of a given element. This allows the concentration of elements in the gemstone to be determined.

The full LA-ICP-MS system used at GIA is shown in figure 4, and a diagram illustrating the general process of analyzing a gemstone by LA-ICP-MS is shown in figure 5. One of the major advantages of LA-ICP-MS is the ability to analyze nearly the entire periodic table, including particularly important elements in the gemological laboratory such as beryllium.

The LIBS technique also relies on the use of a laser ablation unit, but its principle of measuring chemistry is fundamentally different. In the process of laser ablation, a small plasma is generated at the surface of the material being analyzed. As the plasma cools and condenses, light is emitted within micro-to milliseconds after the laser pulse. Similar to XRF, the light's wavelength is related to the energy levels in the atoms that have been ablated, which is different for each element. By pointing a fiber-optic probe at the ablation site and connecting this to one or more spectrometers, the spectrum of light emitted following ablation is monitored. Every ablation shot yields an emission spectrum, which contains information regarding the composition of the material being ablated. In general, LIBS is very powerful at detecting the major elements in a sample, as well as light elements (such as hydrogen, lithium, beryllium, and sodium) at low concentrations (parts-per-million levels or lower). The intensities of the element-specific emission lines are a function of the concentra-

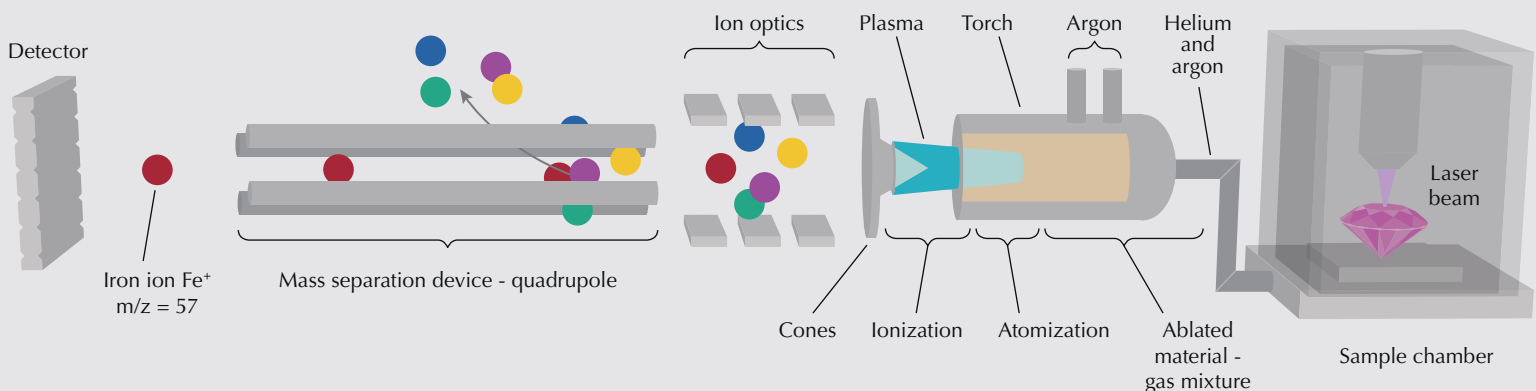
tion of the element, so LIBS data can, in some cases, be turned into quantitative data. In other cases, it can be used for a rapid presence/absence decision, such as the presence of beryllium in corundum.

## TRACE AND MAJOR ELEMENT CHEMISTRY IN THE GEMOLOGICAL LABORATORY

**Qualitative XRF Applications.** Some of the most basic applications of XRF in a gemological laboratory involve simple qualitative analysis to ascertain the presence or absence of certain chemical elements that can identify treatments.

*Glass-Filled Rubies.* One of the most common applications of XRF is the detection of lead glass-filled rubies. Highly fractured and included ruby can be treated with lead glass, which fills fractures and effectively hides them by closely matching the refractive index of corundum. Lead glass filling can often be detected using a gemological microscope

Figure 5. The process of chemical analysis using an LA-ICP-MS system, shown from right to left. Material is laser-ablated from a gemstone in the sample chamber. The ablated material is carried to the argon plasma (temperature of around 10000 K) by helium gas, where it is atomized and ionized. Positively charged ions from the sample pass through a series of cones and are focused into a beam electronically through a series of ion optics. A tunable quadrupole magnet selectively filters the isotope of interest by targeting a specific mass-to-charge ratio ( $m/z$ ), delivering all ions with that value to the detector.





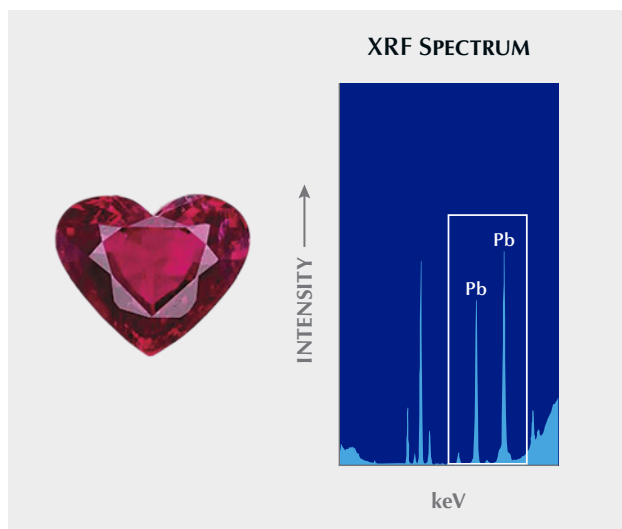


Figure 6. This lead glass-filled ruby displayed the characteristic X-ray fluorescence of lead in its XRF spectrum, indicating the presence of the treatment.

to observe gas bubbles in the glass-filled fractures, luster differences at the surface of the stone, or blue or orange flashes. However, glass-filled rubies often have significant clarity issues which can make these microscopic observations difficult, driving the need for chemical analysis. With XRF, this is done by simply observing the emission associated with lead, which is readily detected in the XRF spectrum (figure 6). Additionally, some recent clarity treatments use glasses with heavy metals other than lead, such as zinc (Sohrabi and Cooper, 2023). In

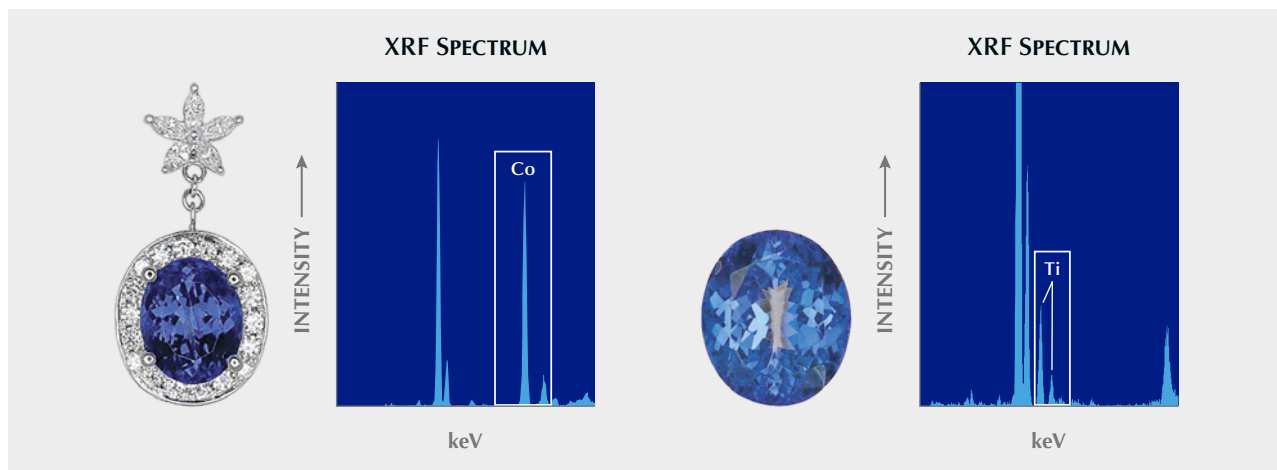
these cases, XRF's ability to identify specific elements becomes even more important.

**Coated Tanzanite.** Another qualitative application of XRF is the detection of coatings on tanzanite (McClure and Shen, 2008). Some tanzanite or zoisite with low color saturation can undergo significant color enhancement by adding a thin layer of cobalt or titanium on the stone's pavilion. While the coating is not permanent and can often be detected by observing visible wear in the microscope, any fresh, unworn applications of this coating can be confirmed by testing the pavilion with XRF (figure 7). High intensities of titanium or cobalt provide definitive proof of this treatment, as natural tanzanite has low concentrations of these elements. A similar treatment determination that relies on qualitative XRF is the detection of strong potassium peaks in Zachery-treated turquoise (Fritsch et al., 1999).

Other qualitative applications of XRF include the detection of color-causing elements in stones where certain variety designations require that the color be caused by specific chromophores. XRF analysis is important for verifying the presence of copper in tourmaline. This separates Paraíba-type tourmaline from iron-colored indicolite, which sometimes has similar colors at lower levels of blue saturation.

**Quantitative Applications of XRF.** While XRF is often described as semiquantitative, proper calibration of the instrument using well-characterized standards can

Figure 7. XRF can detect cobalt- or titanium-coated tanzanite. The presence of characteristic X-ray fluorescence of cobalt (left) or titanium (right) provides strong evidence that the stone has been coated with these elements.



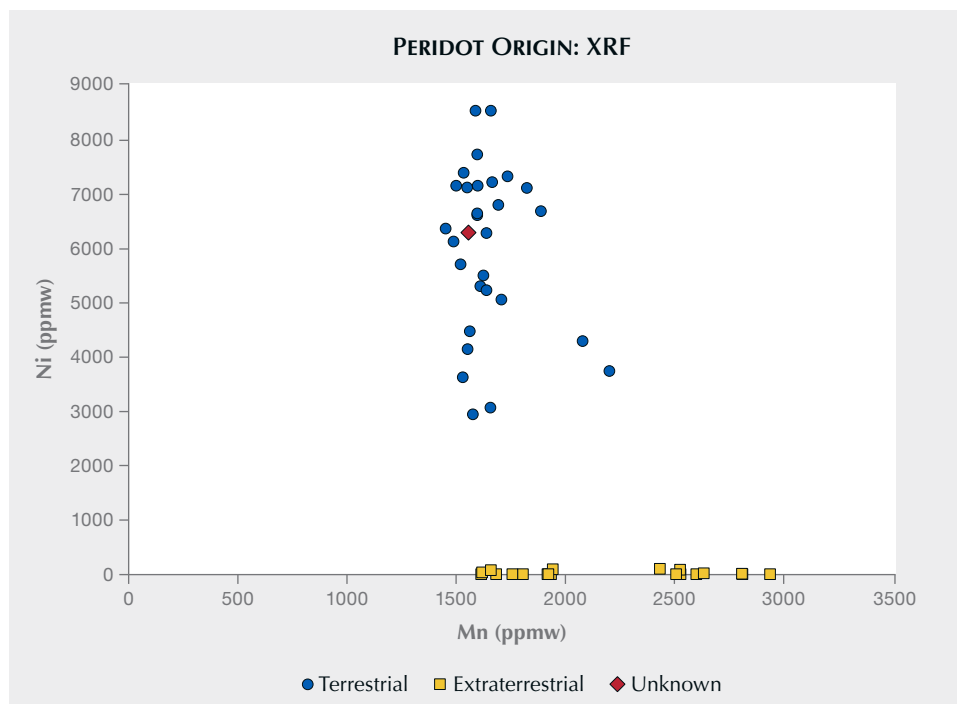


Figure 8. Comparison of nickel vs. manganese in terrestrial and extraterrestrial gem-quality peridot tested by GIA, generated using XRF data. This plot shows that peridot from pallasitic meteorites contains much less nickel than terrestrial peridot. The red diamond shape represents a peridot of unknown origin submitted to the lab. The peridot's placement in the terrestrial peridot field confirms its origin.

allow fully quantitative chemical analyses. XRF does not cover the entire periodic table, but it is frequently used for quantitative analyses, especially for geochemical testing facilities providing whole-rock analysis for mineral exploration and academic studies.

**Pallasitic Peridot.** Pallasitic meteorites consist of a matrix of iron-nickel metal with gemmy peridot that can be extracted and is sometimes faceted as a collector stone. Shen et al. (2011) demonstrated that LA-ICP-MS could be used to separate extraterrestrial pallasitic peridot from terrestrial peridot based on lithium, vanadium, manganese, cobalt, nickel, and zinc concentrations. XRF can also be used to identify pallasitic peridot and separate it from terrestrial peridot by measuring the nickel content (figure 8). Terrestrial, gem-quality green peridot tested by GIA to date contains nickel above ~3000 ppmw, though some terrestrial skarn-related near-colorless gem-quality forsterite contains lower nickel. However, the iron-nickel metal in pallasitic meteorites sequesters most of the nickel, effectively leaving the pallasitic peridot nickel-free.

**Geographic Origin by XRF.** One of the most important uses of XRF and LA-ICP-MS in gemological laboratories is in determining the geographic origin of gemstones. LA-ICP-MS, which will be discussed in

more detail below, is generally the preferred method due to its higher precision, lower detection limits, potentially greater accuracy, and ability to detect light elements. In some cases, however, XRF can be used for geographic origin calls. Although XRF data does not distinguish between as many emerald localities as LA-ICP-MS, it has proven highly effective in identifying emeralds from Colombia and Zambia, which represent the majority submitted to GIA.

Colombian emerald often displays distinct inclusion scenes, especially jagged three-phase fluid inclusions but sometimes pyrite, carbonaceous shale, and rare but diagnostic parisite. However, there is some overlap in their inclusions with other lower-iron metamorphic- or metasomatic-type emeralds from Afghanistan, China, and Musakashi (a Zambian deposit). Likewise, emerald from the major Zambian deposit at Kafubu shows overlap with the inclusion scenes in Brazil, Russia, Ethiopia, and others (Saeseaw et al., 2019). While LA-ICP-MS measurements can confidently identify these and most other origins, XRF can distinguish two major sources by their low iron content (Colombia) or their high iron and cesium contents (Kafubu). For all other origins besides Colombia and Kafubu, there is significant overlap in the XRF trace element data. These other origin calls require the higher precision and lower detection limits for other elements afforded by LA-ICP-MS.

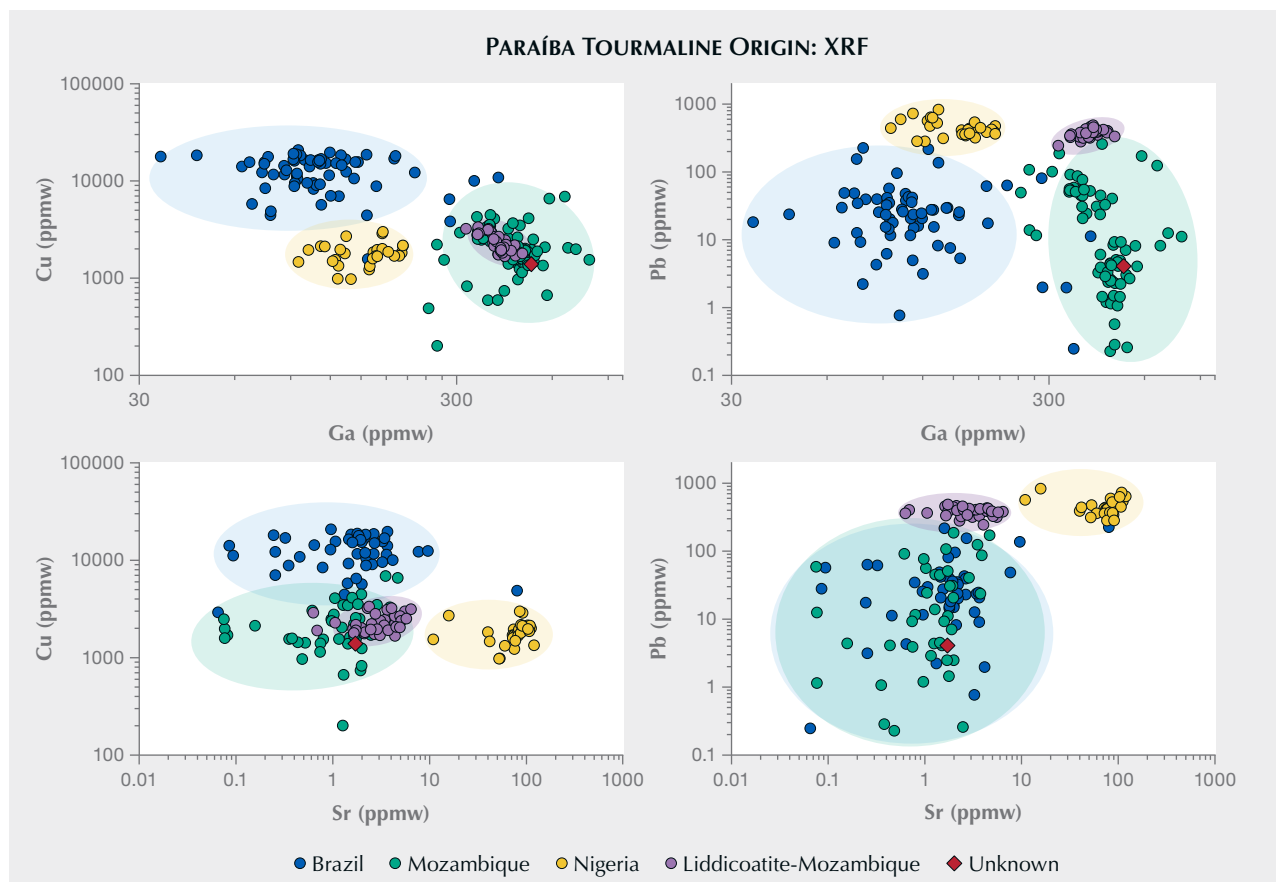


Figure 9. 2D scatter plots of trace elements, generated using XRF, can distinguish the majority of Paraíba tourmalines mined in Brazil, Mozambique, and Nigeria. In these plots, the red diamond shape represents the analysis of a Paraíba tourmaline of unknown origin. Its position in the plots confirms a Mozambique origin.

Although geographic origin determination of Paraíba-type tourmaline is often done by LA-ICP-MS, figure 9 shows that measuring their copper, gallium, and strontium contents using XRF can also be useful. In general, Paraíba tourmaline from Brazil contains higher concentrations of copper and lower concentrations of gallium, strontium, and lead. Non-liddicoatite Paraíba tourmaline from Mozambique contains higher concentrations of gallium and lower concentrations of copper, strontium, and lead. Liddicoatite Paraíba tourmaline from Mozambique contains higher concentrations of lead and gallium and lower concentrations of copper and strontium. Nigerian Paraíba tourmaline contains higher concentrations of strontium and lead and lower concentrations of copper and gallium. The four 2D scatter plots in figure 9 effectively separate the majority of Paraíba tourmaline from different localities.

*Pearl Identification with XRF.* Research has shown that strontium and manganese are excellent discrim-

inators for distinguishing saltwater from freshwater natural and cultured pearls using LA-ICP-MS data (Karampelas et al., 2019). These elements can also be measured accurately using XRF, offering a fast, non-destructive, and reliable alternative to LA-ICP-MS for differentiation. Figure 10 illustrates the strontium vs. manganese distribution in saltwater and freshwater pearls. Freshwater pearls typically exhibit higher manganese and lower strontium concentrations, while saltwater pearls show lower manganese and higher strontium. A decision boundary generated using machine learning algorithms ensures reliable and efficient separation during the analytical process.

*Precious Metal Testing.* Quantitative XRF is widely used to verify precious metal content in jewelry and even to detect plating. Alloys used in jewelry primarily consist of gold, platinum, silver, copper, nickel, cobalt, and zinc, with minor additions of palladium, rhodium, ruthenium, and iridium as coatings or alloy components. Other elements may be incorporated



into alloys to enhance their chemical and physical properties, including corrosion resistance, ductility, hardness, and surface quality.

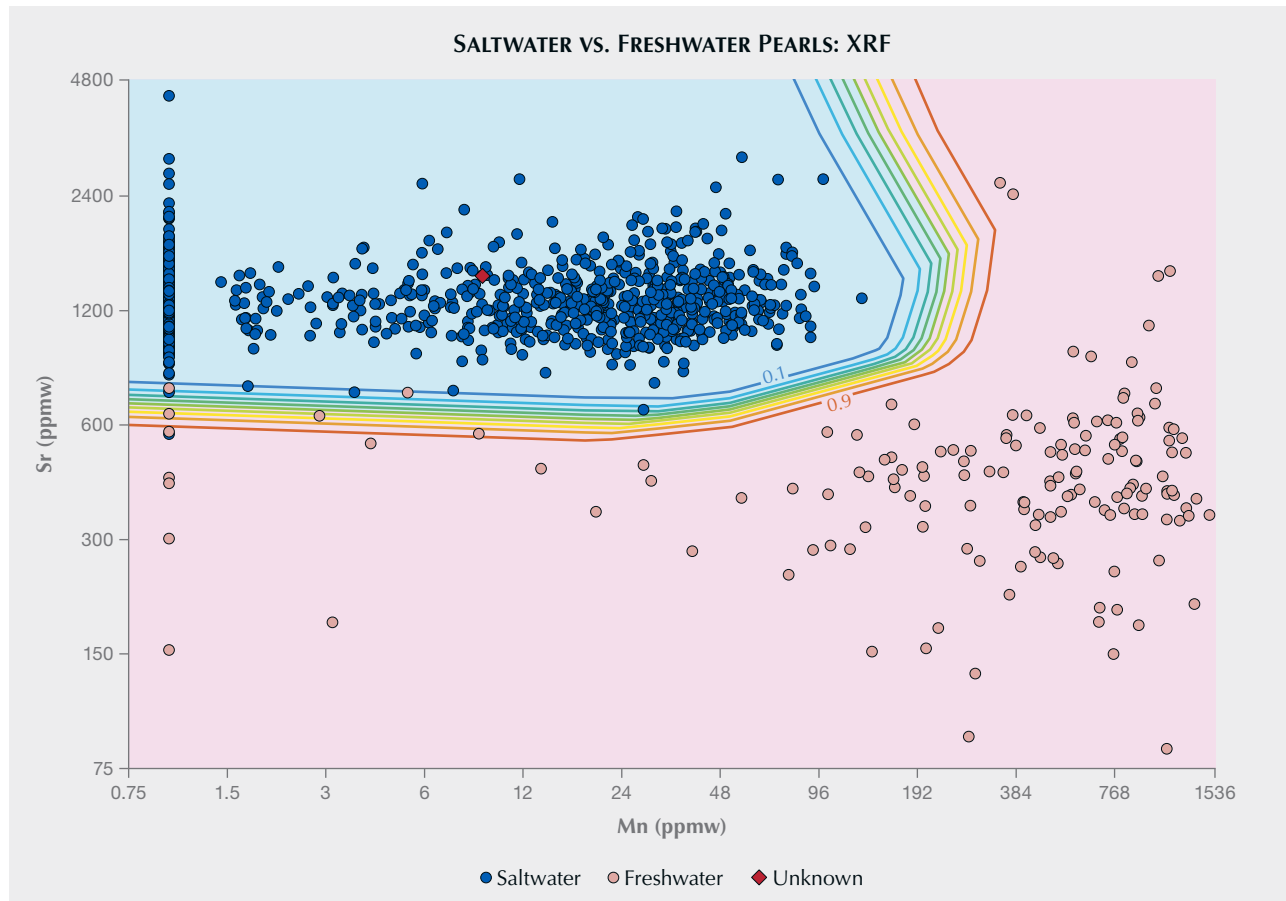
XRF can accurately measure the major components of common gold alloys (Mercer, 1992). XRF can also detect gold plating, often through measurement of the base metal being plated or other metals plated between the gold and base metal such as nickel. Additionally, different X-rays emitted by the gold in a piece of jewelry are absorbed differently by gold and other metals in an alloy. X-rays from a thin layer of gold will travel through less gold before leaving the sample. This means there will be a difference be-

tween the spectrum for gold in a thin layer (i.e., a plating) and the spectrum for a solid piece of gold, which can also be used as an indicator of plating.

#### Applications of LA-ICP-MS in Gemological Testing.

While XRF offers rapid data acquisition, ease of use, and fully nondestructive analysis, LA-ICP-MS has major advantages over XRF in a gemological laboratory. The first is significantly increased sensitivity for essentially all trace elements. In other words, LA-ICP-MS can detect much smaller concentrations of trace elements with greater analytical precision across the periodic table. Detection limits for XRF

Figure 10. Plot distinguishing saltwater from freshwater pearls, generated using XRF data, in which a decision boundary has been determined using machine learning algorithms. Data points to the right of the red line (0.9) are classified as freshwater pearls, with a probability greater than 90%. Data points to the left of the blue line (0.1) are classified as saltwater pearls, with a less than 10% probability of being freshwater. Data points between the red and blue lines are considered questionable and require further examination. The red diamond shape represents a pearl of unknown origin; its position confirms a saltwater origin. Note that the data points in a straight vertical line on the left side contain no detectable manganese; their manganese values were assigned as the assumed detection limit for XRF (1 ppmw) so that these data could be visualized using a log base 2 scale.



generally range from around 1000 ppm for lighter elements to tens of ppm for mid-range elements and around 1 ppm for very heavy elements. Detection limits with LA-ICP-MS are generally below 1 ppm for most elements and down to several parts per billion (ppb) for many of the heavier elements. Another advantage is the ability of LA-ICP-MS to measure light elements that simply cannot be detected by XRF. Light elements such as lithium and beryllium emit lower-energy characteristic X-rays that either cannot reach the XRF detector due to scattering or fall below the low-energy limit of the detector. Even elements like sodium and magnesium can generally only be measured at weight % levels (greater than approximately 10000 ppm) due to these restrictions. LA-ICP-MS, on the other hand, is capable of measuring light elements down to lithium at ppm or sub-ppm levels.

One major distinction from XRF is that LA-ICP-MS is a microanalytical technique that samples very small areas around tens of micrometers. On the other hand, XRF is more of a bulk analysis method that samples much larger surface areas, typically on the order of 1–5 mm<sup>2</sup>, so care must be taken in choosing the technique that provides the appropriate level of spatial analysis. This could be an important consideration in the analysis of single-crystal gemstones with little or no chemical zoning or when analyzing opaque or translucent gems composed of individual cryptocrystalline grains and multiple different minerals in a mechanical mixture.

*Beryllium Diffusion Detection.* In the early 2000s, the colored stone market saw a dramatic influx of sapphire with a pinkish orange to orangy pink “padparadscha”-like color. Given the rarity of natural-color padparadscha sapphire, this new supply raised suspicion in the trade. Subsequent research demonstrated that beryllium diffusion treatment was being used to add an orange or yellow color to pink sapphire by heating these stones at high temperatures in the presence of an external source of beryllium. This produces trapped hole coloration and a padparadscha-like color for pink sapphire (Emmett et al., 2003). Colorless or pale colored sapphire can also be turned to a yellow/orange color, and the color of dark blue sapphires can be lightened significantly with beryllium diffusion. In some of the early production of beryllium-diffused sapphire, orange rims could be identified around the outside of the stone (figure 11). However, beryllium can diffuse very rapidly in corundum at the temperatures used in this process (often

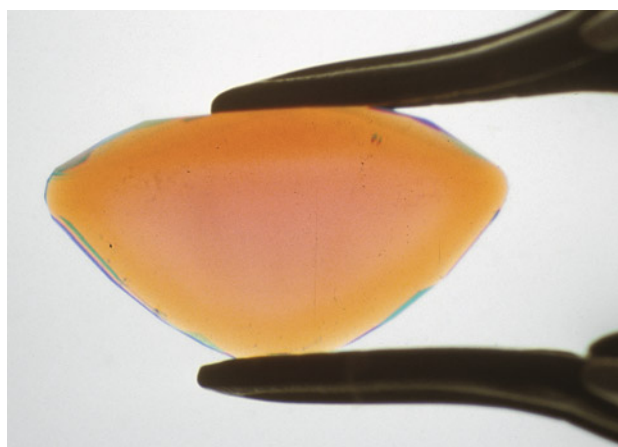


Figure 11. A cross section of a beryllium-diffused sapphire showing a purplish pink core and an orangy pink rim caused by the introduction of beryllium to the corundum structure.

up to 1800°C), so microscopy cannot identify this treatment in many cases.

The only means of analyzing the chemistry of a sapphire in the gem laboratory when this treatment was introduced was by XRF, which cannot detect light elements such as beryllium. Commercially available techniques being used in other fields at the time included LA-ICP-MS and secondary ion mass spectrometry (SIMS). While SIMS is capable of producing exceptionally high-quality data with detection limits much lower than LA-ICP-MS, analysis is very time-consuming and these instruments are very complicated, often requiring a PhD-level scientist just for daily operation of the instrument. SIMS is also a much more significant investment, easily costing over \$1 million just to purchase the instrument.

For this reason, LA-ICP-MS, which can routinely detect beryllium at levels down to 0.1 ppma, was introduced into many gemological laboratories for the sole purpose, at least initially, of identifying beryllium diffusion in ruby and sapphire. Figure 12 shows a laser ablation profile seen when processing LA-ICP-MS data for a beryllium-diffused sapphire with about 10 ppma of beryllium present at the stone’s girdle. LIBS can also be used for beryllium detection, as it is particularly well suited for the light elements. LIBS has the advantage of being less destructive than LA-ICP-MS, as less ablation is required, but it has poorer detection limits and quantification is more challenging.

*Geographic Origin Determination.* LA-ICP-MS is also an exceptional tool in establishing geographic

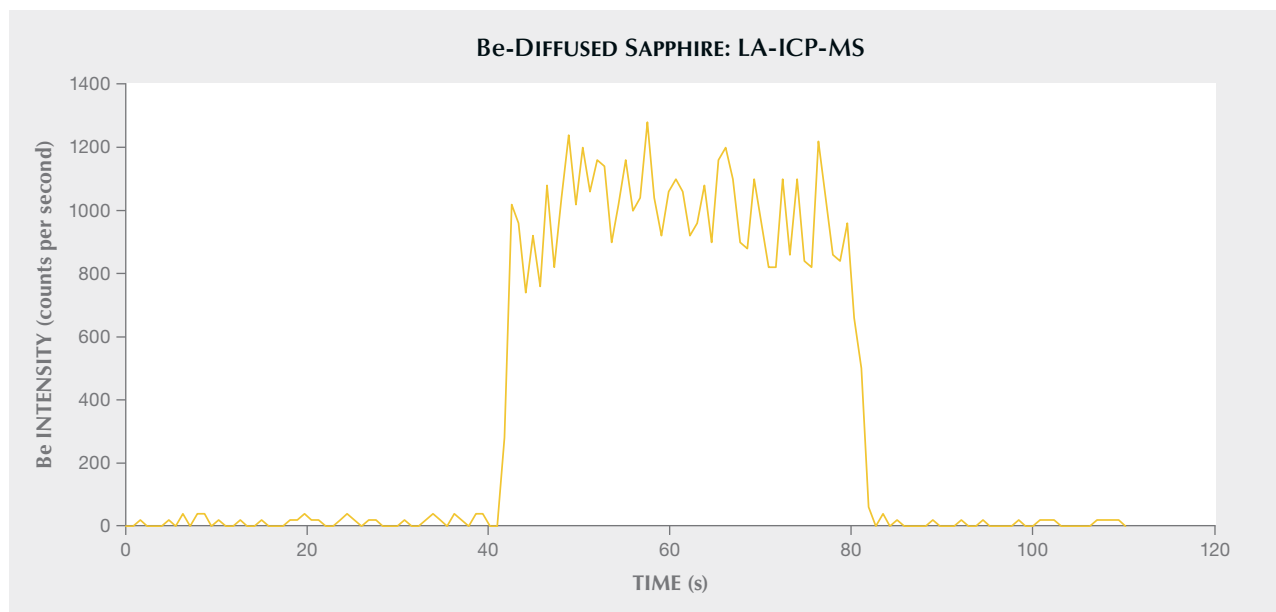


Figure 12. Laser ablation profile of an LA-ICP-MS analysis of a beryllium-diffused sapphire. Ablation begins at the 40 s mark, indicated by a significant increase in beryllium intensity as the laser shutter opens and the laser begins to interact with the stone. Ablation ceases at the 80 s mark, indicated by a rapid decline in the beryllium signal to the gas background level. The intervals from 0 to 40 s and from 80 to 120 s represent the gas background.

origin. The major origin applications currently involve sapphire (Palke et al., 2019a), ruby (Palke et al., 2019b), emerald (Saeseaw et al., 2019), Paraíba tourmaline (Katsurada et al., 2019), alexandrite (Sun et al., 2019a), and red/pink spinel. Research is ongoing to expand the use of LA-ICP-MS for origin analysis of demantoid, blue spinel, peridot, and opal.

Figure 13 shows 2D plots of various trace elements used for geographic origin determination of Paraíba tourmaline. Samples sourced from Brazil, Mozambique, and Nigeria often have similar colors and inclusions, making it essentially impossible to pinpoint their origin using conventional gemological instruments. While the origin of some Paraíba tourmaline can be identified with quantitative XRF analysis (see above), in many cases LA-ICP-MS is needed. The higher precision of LA-ICP-MS affords a higher confidence in trace element measurements, allowing a conclusive origin call for some borderline cases. In addition to the main trace elements used for Paraíba origin determination (copper, gallium, lead, and strontium), other trace elements such as tin and zinc can be useful. These are usually at concentrations too low to be detected by XRF. The chemical trends distinguishing these geographic origins are shown in figure 13. Generally, Paraíba tourmaline from Brazil is characterized by higher concentrations of copper and zinc and lower concentrations of gallium, strontium, and lead. In con-

trast, Paraíba tourmaline from Mozambique exhibits higher concentrations of gallium and lower concentrations of copper, zinc, and strontium. Tourmaline from Nigeria shows elevated levels of strontium and lead and reduced levels of copper and gallium. The violet dots in figure 13 represent a separate species of tourmaline, liddicoatite, from Mozambique.

Emerald geographic origin determination is heavily reliant on trace element analysis by LA-ICP-MS. As with Paraíba tourmaline, some emerald origins—specifically those from Colombia and Kafubu, Zambia—can be confidently identified using only XRF. While XRF trace element data is similar in some ways to that obtained by LA-ICP-MS, XRF detects far fewer trace elements in emerald and at much lower precision. For this reason, LA-ICP-MS is necessary to establish origin for emerald from sources other than Colombia and Kafubu. Trace elements measured by LA-ICP-MS for emerald origin primarily include lithium, potassium, vanadium, chromium, iron, rubidium, and cesium, and many of these cannot be measured by XRF with sufficient precision at the concentrations required for accurate origin determination. In almost all cases, an accurate origin conclusion is possible for all major emerald sources using LA-ICP-MS (Saeseaw et al., 2019).

The geographic origin of alexandrite is also largely determined using trace element analysis by



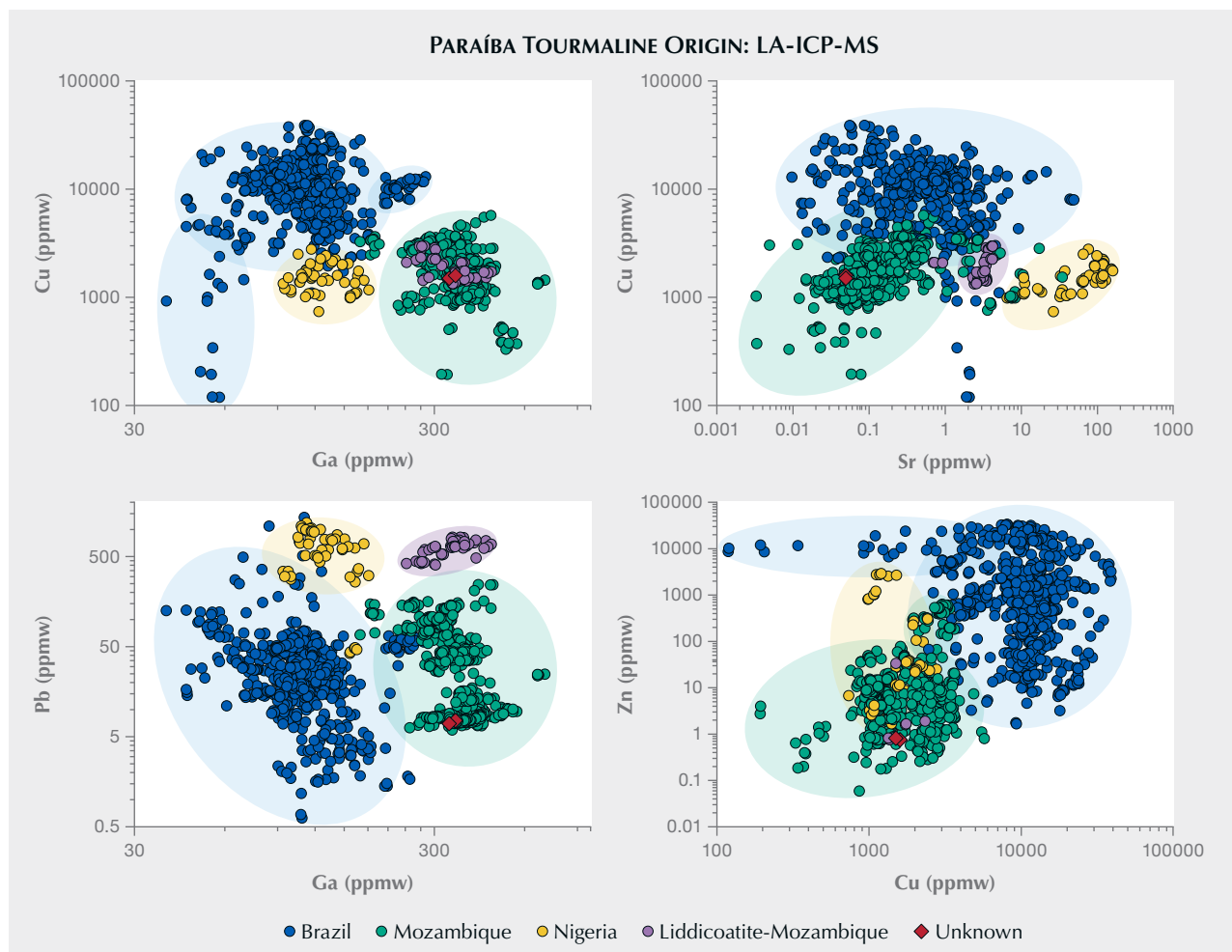


Figure 13. 2D scatter plots of trace elements, generated using LA-ICP-MS, can distinguish the majority of Paraíba tourmalines mined in Brazil, Mozambique, and Nigeria. In these plots, each red diamond shape represents the analysis of a Paraíba tourmaline of unknown origin. Their position in the plots confirms a Mozambique origin.

LA-ICP-MS (Sun et al., 2019a). While there are some general differences in warm/cool color ranges (e.g., incandescent vs. daylight colors) and inclusions between alexandrite from some deposits, there is generally too much overlap to determine origin through standard gemological testing. For instance, Brazilian alexandrite typically occurs with more highly saturated colors, while Sri Lankan has less-saturated colors. But most deposits, including those in Sri Lanka, India, Russia, Tanzania, and Madagascar, can have similar warm/cool colors. The key trace elements for distinguishing alexandrite from different geographic locations by LA-ICP-MS include magnesium, iron, gallium, germanium, tin, boron, vanadium, and chromium. Some of these trace elements are undetectable by XRF (boron and magnesium, except at very high concentrations). Other

trace elements may be detected in some alexandrite, but their concentrations are often too low for accurate XRF analysis. Alexandrite from various countries exhibits distinctive chemical profiles (figure 14). Russian, Zambian, and Zimbabwean alexandrite generally have medium to high concentrations of germanium. Brazilian samples are characterized by high levels of tin and lower concentrations of magnesium and gallium, with some exhibiting extremely low boron levels. Sri Lankan alexandrite is known for its very high gallium concentrations. Tanzanian stones typically show low gallium and medium levels of magnesium and tin. Indian alexandrites are marked by low tin and high vanadium concentrations, while alexandrite from Madagascar is distinguished by low germanium and medium concentrations of gallium and tin. In figure 14, the red

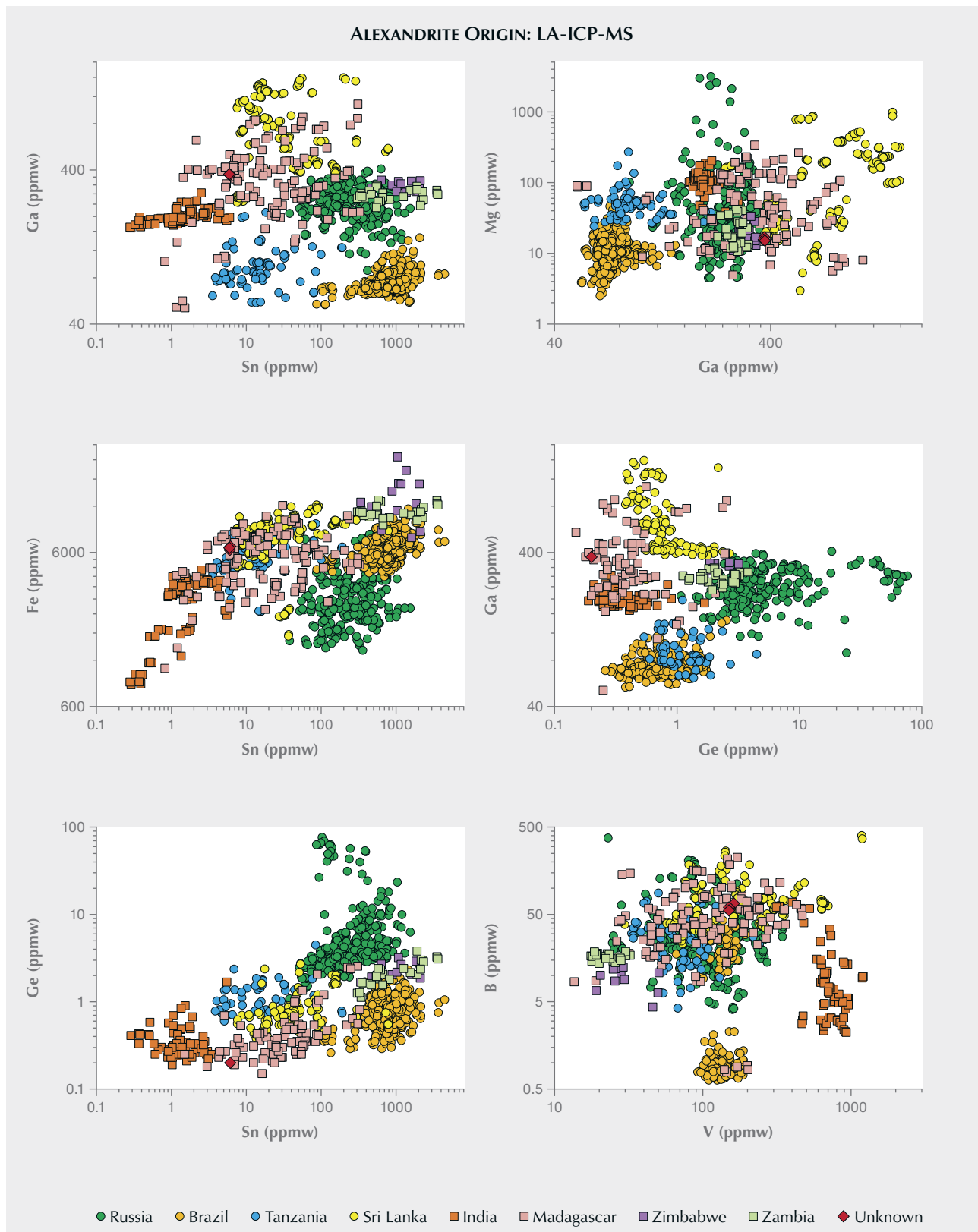


Figure 14. 2D scatter plots of trace elements, generated using LA-ICP-MS, can distinguish the majority of alexandrites mined from different countries. The red diamond shape represents the analysis of an alexandrite of unknown origin. Its position in the plots confirms a Madagascar origin.

---

diamond shape representing a stone of unknown origin is identified as alexandrite from Madagascar based on the analysis of all six plots.

*Ruby and Sapphire Origin Determination.* LA-ICP-MS is a powerful tool for establishing the geographic origin of rubies and sapphires. In many of the examples above (emerald, tourmaline, and tanzanite), there was a clear distinction between the chemical composition of stones from different deposits. For gem corundum (ruby and sapphire), however, trace element chemistry often strongly overlaps between different deposits. This is especially apparent in standard two-dimensional plots where trace element substitution is more limited and constrained to a smaller set of elements (typically magnesium, titanium, vanadium, iron, and gallium for ruby and sapphire). For most ruby and sapphire, microscopic observation of inclusion scenes (and sometimes analyzing spectroscopic features) carries greater weight in geographic origin determination than trace element chemistry. Nonetheless, trace element chemistry can still play an important role in many cases, and various techniques have been developed to enhance the use of trace element chemistry to complement origin data from inclusion features.

Consider a complex magnesium-gallium 2D plot of metamorphic blue sapphires. The data points for the unknown stone are obscured among numerous reference data points, which complicates the stone's origin. To simplify a complex magnesium-gallium 2D plot, additional elements such as vanadium, iron, and titanium are utilized as supplementary dimensions for data filtering.

At GIA's laboratory, the approach to simplifying the comparison with reference data for sapphire and ruby origin is essentially a variation of the k-nearest neighbor statistical approach, in which an unknown is classified by determining which reference data points are closest to it in multidimensional trace element space. This is helpful because humans cannot visualize more than three dimensions. Because we can only see three trace elements at a time in these plots, there is a potential risk of missing valuable information from other trace elements. GIA's approach, referred to as the selective plotting method, essentially reverses the k-nearest neighbor process, allowing simpler visualization of which geographic origins are consistent with the unknown data, with the hope that only one origin will be a strong match (Palke et al., 2019b).

The method is illustrated in figure 15. Using vanadium as the third dimension, we can expand the data from the magnesium-gallium 2D plot into magnesium-gallium-vanadium 3D space. Then we can decide to compare only against data with similar vanadium concentrations by drawing a window around the unknown data in the vertical dimension and excluding reference data outside this window. Then the 3D plot can be projected back onto the magnesium-gallium plot with the data outside the window excluded. The magnesium-gallium plot has far fewer data points than before, making it easier to compare the unknown against our reference data. This process can be repeated by expanding the magnesium-gallium 2D plot into the third dimension with iron and then titanium, again creating windows around the vertical dimension and excluding data in each iteration. The resulting projection back onto the magnesium-gallium plot again has far fewer data points.

The example in figure 15 still does not exclude any origins or produce a "preferred" origin call for this unknown data. However, the process can be repeated, each time with a smaller window around the unknown data in the expanded third dimension. The process used by GIA utilizes coarse, medium, and fine windows that progressively filter the data each time (figure 16). In this example, the unknown sapphire clearly matches our Sri Lankan reference data more closely than any other source when filtering down to the "fine" screen. This process, described in greater detail in Palke et al. (2019a), is used by GIA for ruby, sapphire, emerald, alexandrite, and spinel.

*Origin Determination of Freshwater Pearls Using LA-ICP-MS.* LA-ICP-MS excels at quantifying both light elements (e.g., sodium and magnesium) as well as heavier elements (e.g., barium), making it an ideal tool for pearl analysis. LA-ICP-MS can distinguish the origins of various freshwater pearls, including American natural pearls, American cultured pearls, and Chinese cultured pearls, by analyzing trace elements such as sodium, magnesium, manganese, strontium, and barium (Homkrajac et al., 2019). As illustrated in figure 17 (A and B), American natural pearls typically exhibit lower concentrations of manganese, sodium, strontium, and barium compared to other freshwater pearls, while American cultured pearls are characterized by higher levels of manganese, strontium, and barium



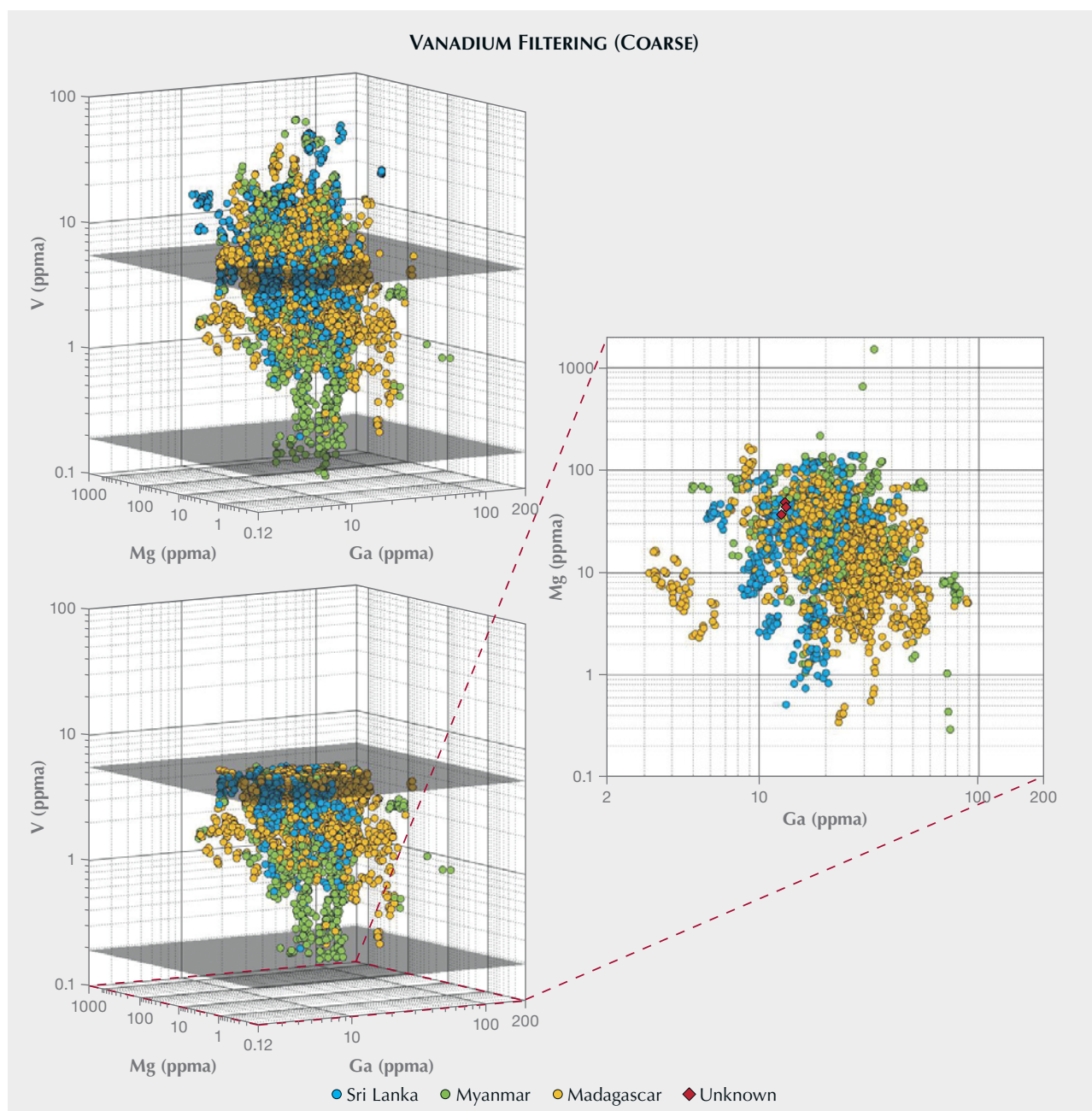


Figure 15. Data filtered using vanadium as the third dimension with a coarse (large) filtering window, simplifying projections back onto the magnesium-gallium 2D plot.

as well as moderate levels of sodium. Chinese cultured pearls, on the other hand, show elevated sodium and strontium levels but lower manganese and barium.

A practical method to clearly visualize and easily interpret this data employs a combination of machine learning techniques. By using principal component analysis (PCA; Abdi and Williams, 2010) for

dimension reduction and a feed-forward neural network (Mishra and Gupta, 2017) for classification, the five-dimensional data space—comprising the elements sodium, magnesium, manganese, strontium, and barium—can be effectively projected into a two-dimensional space. This approach not only simplifies the data but also defines clear decision regions for more straightforward data interpretation. Tech-



Figure 16. Visualization of the simultaneous multidimensional filtering process for metamorphic blue sapphire plots. A: The initial magnesium-gallium 2D plot prior to filtering. B: The magnesium-gallium 2D plot after coarse filtering using vanadium, iron, and titanium. C: The magnesium-gallium 2D plot after medium filtering. D: The magnesium-gallium 2D plot after fine filtering.

niques like PCA are another way of approaching the problem of visualization of multidimensional data, similar to the selective plotting method described above. Figure 17C displays the decision regions for reference freshwater pearl data mapped onto two

principal component axes. Data points within the light red region are likely classified as American natural pearls. Similarly, data points within the light green region are likely classified as American cultured pearls and those within the yellow region as

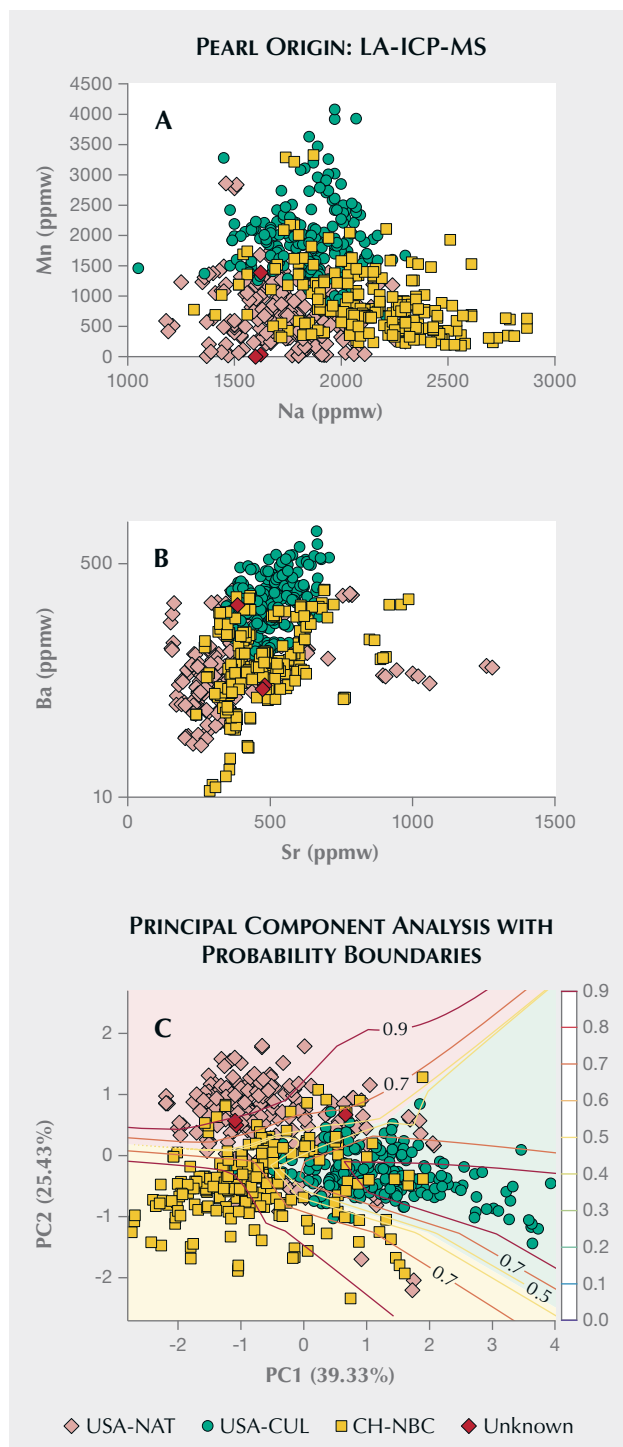


Figure 17. A and B: 2D scatter plots of pearls from three origins: American natural (USA-NAT), American cultured (USA-CUL), and Chinese cultured (CH-NBC) (Homkrajae et al., 2019). C: Principal component analysis, achieved by transforming five-dimensional data (representing five elements) using a projection matrix onto a two-dimensional subspace. The x-axis (first principal component) accounts for 39.33% of the information (“explained variance”) from the original dataset, while the y-axis (second principal component) captures an additional 25.43%. The plot incorporates probability decision boundaries. For each pearl type, data points within the orange to red line boundary (indicating a 0.7–0.9 threshold) are classified as belonging to their respective categories, with a classification probability exceeding 70–90%. Three red diamond shapes represent chemical data points for an unclassified pearl.

roduces certain trade-offs. The reduction in dimensionality through principal component analysis, for example, does not preserve the full variance of the original data structure, capturing only 64.76% of the total variance as shown in figure 17C. Because principal component analysis is restricted to linear transformations, it does not capture complex non-linear patterns present in the data. An alternative approach involves applying a different machine learning technique called a deep feed-forward neural network directly to the original dataset. This method can potentially improve classification accuracy but at the expense of interpretability and the ease of visualization.

*Chemical Mapping on Gemstones with LA-ICP-MS.* LA-ICP-MS is typically used for localized analysis, obtaining elemental information from a microscopic area on a gemstone. However, this technique can also be utilized to characterize the distribution of chemical elements over larger areas, thereby enhancing the comprehensive study of gemstones (Zaw et al., 2015).

For instance, by ablating along parallel lines to cover a substantial rectangular area, one can examine the distribution of associated chemical elements (titanium, tantalum, niobium, tungsten, and thorium) within the cloud-like inclusions of a metamorphic blue sapphire. This approach aids in understanding the sapphire’s growth process and environment and helps identify the nature of the inclusions. Similarly, elemental mapping of a cultured pearl’s cross section can reveal variations in

Chinese. The unknown pearls, represented by red diamond shapes across the plots, are classified as American natural pearls.

While the combined use of machine learning methods enhances the interpretability of results, it is important to acknowledge that this approach in-



elemental density across different concentric growth layers (see figure 18), offering valuable insights into the pearl's growth process and potentially the geographic environment in which it grew. Note, however, that this mapping would leave significant, eye-visible marks on a stone and is not suitable for gems submitted to the lab for reports.

**Materials Identification.** LA-ICP-MS and even XRF can be very useful for identifying gem materials that are challenging to determine using standard gemological techniques. For instance, LA-ICP-MS can separate various garnet species such as pyrope, pyrope-almandine, almandine, almandine spessartine, spessartine, and pyrope-spessartine by accurately measuring the mixture of pyrope-almandine-spessartine end members in the stone. A similar process can be followed for tourmaline species, as described by Sun et al. (2019b).

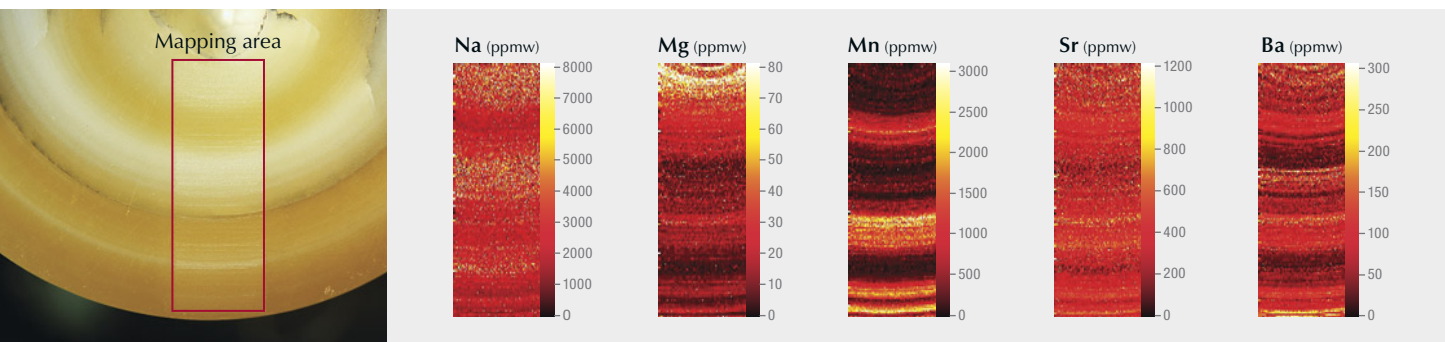
In some cases, gem species are encountered that do not match any known gem materials based on results from standard gemological testing. In these situations, LA-ICP-MS can provide a relatively quick chemical measurement to help identify the gem's species. For instance, LeCroy and Palke (2024) recently used the technique to identify a faceted stone submitted to GIA as titanoholtite, a member of the dumortierite supergroup heretofore observed only as small, non-gemmy crystals from a pegmatite in Poland. XRF can achieve similar results in many cases, but its inability to measure light elements makes LA-ICP-MS the more reliable tool.

LA-ICP-MS also excels at measuring both trace, minor, and major element concentrations in inclusions when they are exposed at the surface. For instance, identifying the various inclusions in the

black topaz shown in figure 19A can be particularly challenging. Raman spectroscopy can effectively identify certain inclusions in this mineral specimen, such as colorless fluorite, reddish brown flaky mica, and magnetite, as shown in figure 19B. However, some inclusions are so rare that their Raman spectra are not well established for comparison, as is the case with the black inclusions from the same specimen shown in figure 19C. In this case, LA-ICP-MS can be employed to conduct precise chemical element analysis of these inclusions. The computed chemical molecular formula of the inclusion is quite complex:  $(\text{Ca}_{0.07}, \text{Ti}_{0.07}, \text{Mn}_{0.19}, \text{Fe}^{3+}_{0.62}, \text{Zr}_{0.04}, \text{Nb}_{0.46}, \text{Mo}_{0.02}, \text{Ta}_{0.01}, \text{W}_{0.43}, \text{others}_{0.03})_{1.95}\text{O}_4$ . When combined with Raman spectroscopy, this analysis identifies the inclusion as a variety of the mineral ixiolite, sometimes informally referred to as wolframioixiolite, a mineral primarily composed of manganese, niobium, and tungsten. While LA-ICP-MS is not expected to give results as accurate as EPMA due to difficulties with non-matrix-matched standardization, in most cases mineral formulas are produced that closely match the expected stoichiometry constraints for the expected mineral, improving confidence in the accuracy of chemical measurements.

**Comparison of LA-ICP-MS, LIBS, and XRF.** LA-ICP-MS and XRF are both widely used in gemological laboratories. A less commonly used technique is LIBS, which shares some similarities with LA-ICP-MS and is even built into some of those systems. Each technique has some advantages and disadvantages. In terms of being able to accurately and precisely determine concentrations of most elements with high spatial resolution, LA-ICP-MS is by far the best tool. XRF has the advantage of being the only of these

Figure 18. LA-ICP-MS elemental maps of a cross section of a cultured pearl. The red rectangle indicates the area mapped, measuring  $1200 \times 3400 \mu\text{m}$ .





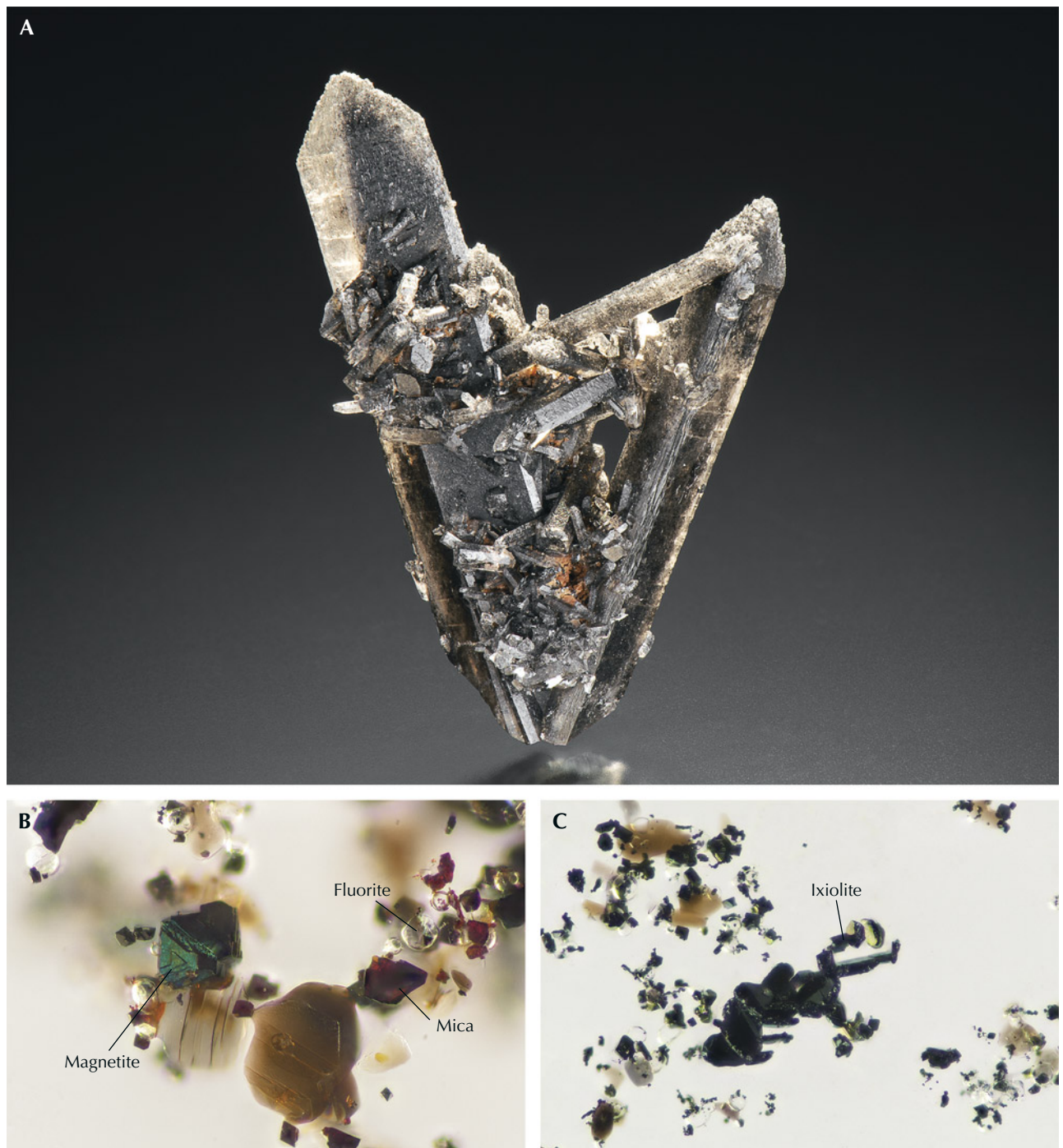


Figure 19. A: A black topaz crystal specimen from the Thomas Mountains in Utah, measuring  $24.80 \times 17.92 \times 12.29$  mm. Photo by Kevin Schumacher. B: Inclusions of black magnetite, colorless fluorite, and flaky mica in the black topaz. C: Clusters of tabular ixiolite. From Muyal et al. (2019); fields of view 0.288 mm (B) and 0.36 mm (C).

methods that is truly nondestructive. LIBS offers the same spatial resolution advantages as LA-ICP-MS but is considerably faster, with less stringent requirements for laboratory conditions.

On the other hand, LA-ICP-MS systems are the most expensive to purchase and operate, with a potentially five to ten times higher cost than LIBS and XRF systems. LIBS data are considerably more

challenging to quantify than LA-ICP-MS, and the usefulness of LIBS for trace element analysis is limited to light elements. The XRF systems typically employed at gemological laboratories, as described above, cannot perform microanalytical analysis and struggle with lighter elements. There are, however, some micro-XRF instruments available on the market that can scan with a spatial resolution of approximately 20  $\mu\text{m}$ .

Detection limits are also significantly lower for LA-ICP-MS measurements than for XRF. LIBS may have fairly low detection limits in the ppm range for light elements, close to but generally higher than LA-ICP-MS measurements. However, detection limits for heavier elements can be closer to hundreds or thousands of ppm for LIBS, putting the technique at a disadvantage compared to LA-ICP-MS.

## SUMMARY

As identification demands have grown more complex over the last few decades, gemological laboratories have had to adopt progressively more advanced analytical instrumentation. Measurements of a gemstone's chemical composition have proven to be of paramount importance in many ways. XRF was the first chemical analysis technique introduced to most gemological laboratories. Later, chemical measurement techniques were supplemented with LIBS and more importantly LA-ICP-MS with the introduction of beryllium-diffused corundum and the growing importance of geographic origin determination. While LA-ICP-MS can be a challenging instrument to operate and maintain, the modern gem trade often relies on laboratories to use this technology for accurate gemstone identification.

### ABOUT THE AUTHORS

Ziyin Sun is a senior research associate, and Dr. Aaron Palke is senior manager of research, at GIA in Carlsbad. Dr. Michael Jollands is a senior research scientist at GIA in New York.

### ACKNOWLEDGMENTS

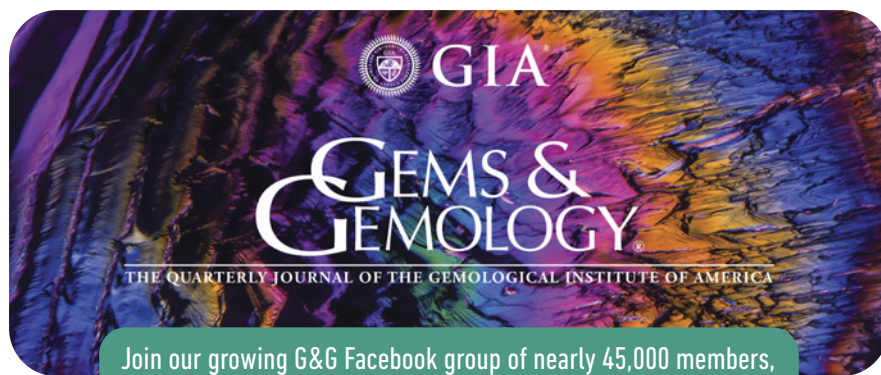
The authors are deeply indebted to many years of guidance and collaboration with many researchers and gemologists while work-

ing at GIA, including Shane McClure, Nathan Renfro, John Emmett, George Rossman, Artitaya Homkrajae, Tom Moses, and Sudarat Saeseaw, among others, as well as GIA's field gemology department for providing access to samples with known provenance that has made all of this research possible. Many thanks to Chunhui Zhou for providing the pearl sample for elemental mapping using LA-ICP-MS.

## REFERENCES

- Abdi H., Williams L.J. (2010) Principal component analysis. *WIREs Computational Statistics*, Vol. 2, No. 4, pp. 433–459, <http://dx.doi.org/10.1002/wics.101>
- Abduriyim A., Kitawaki H. (2006) Applications of laser ablation-inductively coupled plasma-mass spectrometry (LA-ICP-MS) to gemology. *G&G*, Vol. 42, No. 2, pp. 98–118, <http://dx.doi.org/10.5741/GEMS.42.2.98>
- Eaton-Magaña S., Jones D.C., Turnier R.B., Breeding C.M. (2024) Shining a light on gemstone properties: An exploration of photoluminescence spectroscopy. *G&G*, Vol. 60, No. 4, pp. 494–517, <http://dx.doi.org/10.5741/GEMS.60.4.494>
- Emmett J.L., Scarratt K., McClure S.F., Moses T., Douthit T.R., Hughes R., Novak S., Shigley J.E., Wang W., Bordelon O., Kane R.E. (2003) Beryllium diffusion of ruby and sapphire. *G&G*, Vol. 39, No. 2, pp. 84–135, <http://dx.doi.org/10.5741/GEMS.39.2.84>
- He F., Van Espen P.J. (1991) General approach for quantitative energy dispersive X-ray fluorescence analysis based on fundamental parameters. *Analytical Chemistry*, Vol. 63, No. 20, pp. 2237–2244, <http://dx.doi.org/10.1021/ac00020a009>
- Fritsch E., McClure S.F., Ostrooumov M., Andres Y., Moses T., Koivula J.I., Kammerling R.C. (1999) The identification of Zachery-treated turquoise. *G&G*, Vol. 35, No. 1, pp. 4–16, <http://dx.doi.org/10.5741/GEMS.35.1.4>
- Gray A.L. (1985) Solid sample introduction by laser ablation for inductively coupled plasma source mass spectrometry. *Analytyst*, Vol. 110, No. 5, pp. 551–556, <http://dx.doi.org/10.1039/an9851000551>
- Homkrajae A., Sun Z., Blodgett T., Zhou C. (2019) Provenance discrimination of freshwater pearls by LA-ICP-MS and linear discriminant analysis (LDA). *G&G*, Vol. 55, No. 1, pp. 47–60, <http://dx.doi.org/10.5741/GEMS.55.1.47>
- Johnson R.G., King B.S. (1987) Energy-dispersive X-ray fluorescence spectrometry. In P.A. Baedecker, Ed., *U.S. Geological Survey Bulletin 1770: Methods for Geochemical Analysis*, pp. F1–F5.
- Karampelas S., Mohamed F., Abdulla H., Almahmood F., Flammarzi L., Sangsawong S., Alalawi A. (2019) Chemical characteristics of freshwater and saltwater natural and cultured pearls from different bivalves. *Minerals*, Vol. 9, No. 6, article no. 357, <http://dx.doi.org/10.3390/min9060357>

- Katsurada Y., Sun Z., Breeding C.M., Dutrow B.L. (2019) Geographic origin determination of Paraíba tourmaline. *G&G*, Vol. 55, No. 4, pp. 648–659, <http://dx.doi.org/10.5741/GEMS.55.4.648>
- Krzemnicki M.S., Hänni H.A., Walters R.A. (2004) A new method for detecting Be diffusion-treated sapphires: Laser-induced breakdown spectroscopy (LIBS). *G&G*, Vol. 40, No. 4, pp. 314–322, <http://dx.doi.org/10.5741/GEMS.40.4.314>
- Krzemnicki M.S., Pettke T., Hänni H.A. (2006) Perspectives of LIBS in gemstone testing: Analysis of light elements such as beryllium, boron, lithium. GIT International Gem & Jewelry Conference (GIT 2006).
- LeCroy B., Palke A. (2024) Lab Notes: Exceptionally rare titanoholtite. *G&G*, Vol. 60, No. 1, pp. 71–72.
- McClure S.F., Shen A.H. (2008) Coated tanzanite. *G&G*, Vol. 44, No. 2, pp. 142–147, <http://dx.doi.org/10.5741/GEMS.44.2.142>
- McMillan N.J., McManus C.E., Harmon R.S., De Lucia F.C. Jr., Miziolek A.W. (2006) Laser-induced breakdown spectroscopy analysis of complex silicate minerals—beryl. *Analytical and Bioanalytical Chemistry*, Vol. 385, No. 2, pp. 263–271, <http://dx.doi.org/10.1007/s00216-006-0374-9>
- Mercer M.E. (1992) Methods for determining the gold content of jewelry metals. *G&G*, Vol. 28, No. 4, pp. 222–233, <http://dx.doi.org/10.5741/GEMS.28.4.222>
- Mishra C., Gupta D.L. (2017) Deep machine learning and neural networks: An overview. *IAES International Journal of Artificial Intelligence*, Vol. 6, No. 2, pp. 66–73, <http://dx.doi.org/10.11591/ijai.v6.i2.pp66-73>
- Muyal J., Sun Z., Shigley J. (2019) *G&G* Micro-World: Inclusion-rich black topaz from the Thomas Mountains, Utah. *G&G*, Vol. 55, No. 2, pp. 266–269.
- Palke A.C., Saeseaw S., Renfro N.D., Sun Z., McClure S.F. (2019a) Geographic origin determination of ruby. *G&G*, Vol. 55, No. 4, pp. 580–612, <http://dx.doi.org/10.5741/GEMS.55.4.580>
- (2019b) Geographic origin determination of blue sapphire. *G&G*, Vol. 55, No. 4, pp. 536–579, <http://dx.doi.org/10.5741/GEMS.55.4.536>
- Pornwilard M.-M., Hansawek R., Shiowatana J., Siripinyanond A. (2011) Geographical origin classification of gem corundum using elemental fingerprint analysis by laser ablation inductively coupled plasma mass spectrometry. *International Journal of Mass Spectrometry*, Vol. 306, No. 1, pp. 57–62, <http://dx.doi.org/10.1016/j.ijms.2011.06.010>
- Rinaldi R., Llovet X. (2015) Electron probe microanalysis: A review of the past, present, and future. *Microscopy and Microanalysis*, Vol. 21, No. 5, pp. 1053–1069, <http://dx.doi.org/10.1017/S1431927615000409>
- Saeseaw S., Weeramonkhonlert V., Khowpong C., Ng-Pooresatien, N., Sangsawong S., Raynaud V., Ito C. (2015) Cobalt diffusion of natural spinel: A report describing a new treatment on the gem market. *GIA Research News*, June 3, <https://www.gia.edu/doc/Cobalt-Diffusion-in-Spinel-v2.pdf>
- Saeseaw S., Renfro N.D., Palke A.C., Sun Z., McClure S.F. (2019) Geographic origin determination of emerald. *G&G*, Vol. 55, No. 4, pp. 614–646, <http://dx.doi.org/10.5741/GEMS.55.4.614>
- Shen A.H., Koivula J.I., Shigley J.E. (2011) Identification of extra-terrestrial peridot by trace elements. *G&G*, Vol. 47, No. 3, pp. 208–213, <http://dx.doi.org/10.5741/GEMS.47.3.208>
- Sohrabi S., Cooper A. (2023) Lab Notes: Translucent ruby filled with zinc glass. *G&G*, Vol. 59, No. 3, pp. 368–369.
- Sun Z., Palke A.C., Muyal J., DeGhionno D., McClure S.F. (2019a) Geographic origin determination of alexandrite. *G&G*, Vol. 55, No. 4, pp. 660–681, <http://dx.doi.org/10.5741/GEMS.55.4.660>
- Sun Z., Palke A.C., Breeding C.M., Dutrow B.L. (2019b) A new method for determining gem tourmaline species by LA-ICP-MS. *G&G*, Vol. 55, No. 1, pp. 2–17, <http://dx.doi.org/10.5741/GEMS.55.1.2>
- Sylvester P. J., Jackson S.E. (2016) A brief history of laser ablation inductively coupled plasma mass spectrometry (LA-ICP-MS). *Elements*, Vol. 12, No. 5, pp. 307–310, <http://dx.doi.org/10.2113/gselements.12.5.307>
- Zaw K., Sutherland L., Yui T.F., Meffre S., Thu K. (2015) Vanadium-rich ruby and sapphire within Mogok Gemfield, Myanmar: Implications for gem color and genesis. *Mineralium Deposita*, Vol. 50, No. 1, pp. 25–39, <http://dx.doi.org/10.1007/s00126-014-0545-0>



Join our growing G&G Facebook group of nearly 45,000 members, connecting gem enthusiasts from all over the world!

